

# Polytropic Gas Effects in Parker's Solar Wind Model and Coronal Hole Flows

B. K. Shivamoggi<sup>1,2</sup> and L. Pohl<sup>2</sup>

<sup>1</sup>California Institute of Technology, Pasadena, CA 91125

<sup>2</sup>University of Central Florida, Orlando, FL 32816

July 26, 2024

## Abstract

A detailed and systematic investigation of polytropic gas effects in Parker's solar wind model and coronal-hole flows is given. We present a viable equation governing the acceleration of solar wind of a polytropic gas and give its *exact analytical* and numerical solutions and deduce its asymptotic analytic properties (i) near the sun, (ii) far away from the sun, (iii) near the Parker sonic critical point (where the wind speed is equal to the speed of sound in the wind). We proceed to give a detailed and systematic investigation of coronal-hole polytropic gas outflows which contribute to bulk of the solar wind. We will model coronal-hole outflow by considering a single radial stream tube and use phenomenological considerations to represent its rapidly-diverging flow geometry. We give analytical and numerical solutions for this outflow and deduce its asymptotic analytic properties in the three flow regimes above. We find that, in general, the polytropic effects cause the Parker sonic critical point to move closer to the sun than that for the case with isothermal gas. Furthermore, the flow acceleration is found to exhibit (even for an infinitesimal deviation from isothermality of the gas) a *power-law* behavior rather than an exponential-law behavior near the sun or a logarithmic-law behavior far away from the sun, thus implying a certain robustness of the power-law behavior. The Parker sonic critical point is shown to continue to be of *X*-type, hence facilitating a smooth transition from subsonic to supersonic wind flow through the transonic regime. Our analytical and numerical solutions show that the super-radiality of the stream tube causes the Parker sonic critical point to move further down in the corona, and the gas to become more diabatic (the polytropic exponent  $\gamma$  drops further below 5/3), and the flow acceleration to be enhanced further.

# 1 Introduction

Solar wind is a continuous plasma outflow from the sun, the bulk of which emerges from the coronal holes (Sakao et al. 2007). Solar wind carries off a huge amount of angular momentum from the sun while causing a negligible mass loss from the sun. Weak to moderate solar winds are produced by an extended active heating of the corona in the conjunction with high thermal conduction. Parker (1958) pointed out that high-speed solar winds need some additional acceleration mechanism operational beyond the coronal base and gave an ingenious model to continually convert the coronal thermal energy into the kinetic energy of the wind to produce a smooth acceleration of the latter through transonic speeds (i.e., wind speeds near the speed of sound in the wind). The solar wind and its properties have been recorded by the *in-situ* observations (Meyer-Vernet 2007). Incoming data from the Parker Solar Probe has been providing considerable useful information about the solar corona conditions (Fisk and Kasper (2020) and the references thereof), some of which (like the coupling of the solar wind with the solar rotation (Kasper et al. 2019)) can be the cause of faster solar winds (Shivamoggi 2020) via the mechanism of centrifugal driving.

A major assumption in Parker’s original solar wind model (Parker 1958) was that the gas flow occurs under isothermal conditions, i.e., (in standard notation),

$$p = a^2 \rho ,$$

where the speed of sound  $a$  is taken to be constant. On the other hand, the solar wind is found (Boldyrev, Forest, and Egedal 2020) not to cool down as fast as that caused even by an adiabatic expansion, indicating the presence of significant heating in the corona impairing adiabaticity. A polytropic gas model (Parker 1971; Holzer 1979; Keppens and Goedbloed 1999; Shivamoggi, Rollins, and Pohl 2021), described by

$$p = \mathcal{C} \rho^\gamma ,$$

where  $\gamma$  is the polytropic gas exponent,  $1 < \gamma < 5/3$ , and  $\mathcal{C}$  is an arbitrary constant, is suitable for this situation. The formulation given by Holzer (1979) is not in a convenient form and does not facilitate a systematic exploration of polytropic gas effects as well as easy comparison with the isothermal gas results treated by Parker (1958). On the other hand, the formulation of Shivamoggi, Rollins, and Pohl (2021) did not include the effects of solar gravity in estimating the stagnation flow properties in the solar wind and is hence quantitatively not very accurate near the coronal base. The purpose of this paper is to remedy these issues, and to provide a detailed and systematic investigation of polytropic gas effects on the dynamics of the solar wind. Toward this objective we present a viable equation governing the acceleration of solar wind of a polytropic gas and give its *exact analytical* and numerical solutions and deduce its asymptotic analytic properties,

- near the sun,
- far away from the sun,
- near the Parker sonic critical point (where the wind speed is equal to the speed of sound in the wind).

Following Bondi (1952), we formulate the solar wind model for the polytropic gas by introducing the Mach number  $M$  of the flow  $M \equiv v_r/a$ , which turns out to be the optimal variable for describing the polytropic gas flow.

The coronal-hole outflows, which contribute to the bulk of the solar wind, are known to be permeated radially by divergent open unipolar magnetic field lines threading them (Altschuler, Trotter, and Orrall 1972; Krieger, Timothy, and Roelof 1973; Nolte et al. 1976). Furthermore, coronal-hole outflows are found to be super-radial involving rapidly divergent geometries in the sense that the cross-sectional area of a given stream tube in this inner-corona region increases outward from the sun faster than  $r^2$  (that corresponding to a spherical geometry). Recent Parker Solar Probe observations (Bale et al. 2023) indicate the fast solar wind emerges from the coronal holes via the process of magnetic reconnection between the open and closed magnetic field lines (called the *interchange connection*). Kopp and Holzer (1976) and Wang and Sheeley (1990) proposed to model the coronal-hole outflows by suitable super-radial geometries, and the numerical calculations of Kopp and Holzer (1976) showed enhancement of the flow acceleration and hence a transition to supersonic flow closer to the sun.

In order to circumvent the mathematical difficulties posed by an explicit consideration of non-radial flows, we will model a coronal-hole outflow by a magnetic-field aligned infinitesimal radial stream tube, and consider only a single stream tube because it would disrupt radial geometry for the neighboring stream tubes. We may then, on phenomenological grounds, represent the rapidly-diverging geometry of the stream tube by taking the cross-sectional area  $A(r)$  to increase outward from the sun faster than  $r^2$  (that corresponding to a spherical geometry), as described by  $A(r) \sim r^\beta$ ,  $\beta > 2$ . We will use this phenomenological model to provide a detailed and viable theoretical investigation of coronal-hole outflows in a polytropic gas. We will present an equation governing such flows and give its *exact analytical* and numerical solutions, and deduce its asymptotic analytic properties in the three regimes listed previously.

## 2 Solar Wind Model with a Polytropic Gas

Parker's (1958) solar wind model assumes a steady and spherically symmetric radial flow so the flow variables depend only on the radial distance  $r$  from the sun. Furthermore, the flow variables and their derivatives are assumed to vary continuously so there are no shocks anywhere in the region under consideration.

The equations expressing the conservation of mass and momentum balance are (in usual notations):

$$\frac{2}{r} + \frac{1}{\rho} \frac{d\rho}{dr} - \frac{1}{v_r} \frac{dv_r}{dr} = 0, \quad (1)$$

$$\rho v_r \frac{dv_r}{dr} = -\frac{dp}{dr} - \rho \frac{GM_\odot}{r^2}, \quad (2)$$

where  $G$  is the gravitational constant and  $M_\odot$  is the mass of the sun.

We assume the polytropic gas relation,

$$p = C \rho^\gamma, \quad (3)$$

where  $C$  is an arbitrary constant, and  $\gamma$  is the polytropic exponent,  $1 < \gamma < 5/3$ , which characterizes the extent to which conditions within the solar coronal gas

depart from adiabatic conditions ( $\gamma = 5/3$ ) due to coronal heating effects via thermal conduction and wave dissipation (Parker 1960).<sup>1</sup>

Using equations (1)–(3), we obtain,

$$\left(\frac{v_r^2}{a^2} - 1\right) \frac{2v_r}{a^2} \frac{dv_r}{dr} = \frac{4}{r^2} \frac{v_r^2}{a^2} (r - r_*), \quad (4)$$

$a$  is the speed of sound in the gas, and  $r_*$  locates the Parker sonic critical point in the corona where the flow speed equals the local sound speed,

$$a^2 \equiv \frac{dp}{d\rho}, \quad (5a)$$

$$r_* \equiv \frac{GM_\odot}{2a^2}. \quad (5b)$$

We now follow Bondi's (1952) suggestion, in the context of the related accretion disk model, that the polytropic case is best formulated by introducing the Mach number  $M$  of the flow,  $M \equiv v_r/a$ .

Introducing the total energy  $E$ , we have,

$$\frac{v_r^2}{2} + \frac{a^2}{\gamma - 1} - \frac{GM_\odot}{r} = E \equiv \frac{\tilde{a}_0^2}{\gamma - 1}, \quad (6)$$

from which, we obtain:

$$\frac{\tilde{a}_0^2}{a^2} = \frac{1 + \frac{\gamma-1}{2} M^2}{1 + 4 \frac{\gamma-1}{2} \frac{\tilde{r}_{*0}}{r}}, \quad (7)$$

where  $\tilde{r}_{*0} \equiv \frac{GM_\odot}{2\tilde{a}_0^2}$ .

We have,

$$\frac{dM^2}{dr} = \frac{2v_r}{a^2} \frac{dv_r}{dr} - \frac{2v_r^2}{a^3} \frac{da}{dr}. \quad (8)$$

Using (7), (8) leads to,

$$\frac{2v_r}{a^2} \frac{dv_r}{dr} = \left[ \frac{1}{1 + \frac{\gamma-1}{2} M^2} \right] \frac{dM^2}{dr} - M^2 \left[ \frac{4 \frac{\gamma-1}{2} \frac{\tilde{r}_{*0}}{r^2}}{1 + 4 \frac{\gamma-1}{2} \frac{\tilde{r}_{*0}}{r}} \right]. \quad (9)$$

Using (9), (4) leads to,

$$\begin{aligned} & \frac{M^2 - 1}{M^2 \left(1 + \frac{\gamma-1}{2} M^2\right)} \frac{dM^2}{dr} - (M^2 - 1) \left[ \frac{4 \frac{\gamma-1}{2} \frac{\tilde{r}_{*0}}{r^2}}{1 + 4 \frac{\gamma-1}{2} \frac{\tilde{r}_{*0}}{r}} \right] \\ & = \frac{4}{r^2} \left( r - \frac{1 + \frac{\gamma-1}{2} M^2}{1 + 4 \frac{\gamma-1}{2} \frac{\tilde{r}_{*0}}{r}} \tilde{r}_{*0} \right), \end{aligned} \quad (10)$$

or on simplification, the equation governing the polytropic gas flow becomes,

$$\frac{M^2 - 1}{M^2 \left(1 + \frac{\gamma-1}{2} M^2\right)} \frac{dM^2}{dr} = \frac{4}{r^2} \left( r - \frac{\gamma + 1}{2} \frac{1}{1 + 4 \frac{\gamma-1}{2} \frac{\tilde{r}_{*0}}{r}} \tilde{r}_{*0} \right). \quad (11)$$

<sup>1</sup>A more detailed investigation is to make use of a complete energy equation with thermal conduction and heating effects in the solar corona.

Equation (11) is the generalization of Parker (1958) isothermal solar wind flow equation for the polytropic gas, and reduces to the former in the isothermal limit  $\gamma = 1$ .

Observe from equation (10) or (11) that the Parker sonic critical point for a polytropic gas is given by,

$$M^2 = 1: \quad r_* = \frac{\gamma + 1}{2} \frac{1}{1 + 4 \frac{\gamma - 1}{2} \frac{\tilde{r}_{*0}}{r_*}} \tilde{r}_{*0} = 0,$$

or

$$M^2 = 1: \quad r_* = \frac{5 - 3\gamma}{2} \tilde{r}_{*0}. \quad (12a)$$

We may rewrite (12a) as

$$M^2 = 1: \quad r_* = \left[ 1 - \frac{3}{2} (\gamma - 1) \right] \tilde{r}_{*0} < \tilde{r}_{*0}, \quad (12b)$$

which implies that the polytropic effects ( $\gamma > 1$ ) cause the Parker sonic critical point to move closer to the sun (see Figure 1) than that for the case with isothermal gas ( $\gamma = 1: r_* = \tilde{r}_{*0}$ ), in agreement with our previous results (Shivamoggi, Rollins, and Pohl 2021) for the more restricted polytropic gas case.

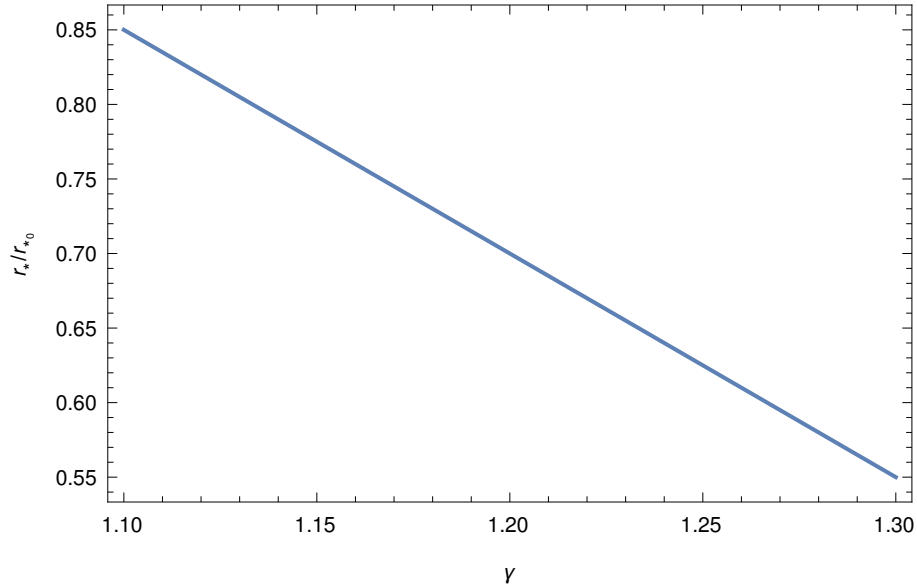


Figure 1: Polytropic effects, as per (12), on the Parker sonic critical point.

### 3 Exact Solution

Upon imposing the boundary condition (12), equation (11) yields the *exact* solution,

$$\begin{aligned}
 & -\log M^2 + \frac{\gamma+1}{\gamma-1} \log\left(\frac{1 + \frac{\gamma-1}{2}M^2}{\frac{\gamma+1}{2}}\right) \\
 &= \frac{3\gamma-5}{\gamma-1} \log\left(\frac{2r}{(5-3\gamma)\tilde{r}_{*0}}\right) + \frac{\gamma+1}{\gamma-1} \log\left(\frac{r + 4\frac{\gamma-1}{2}\tilde{r}_{*0}}{\frac{\gamma+1}{2}\tilde{r}_{*0}}\right). \tag{13}
 \end{aligned}$$

In the isothermal gas limit, ( $\gamma = 1$ ), (13) reduces to the Parker solar wind solution,

$$-\log M^2 + M^2 = 4 \log \frac{r}{\tilde{r}_{*0}} + 4 \frac{\tilde{r}_{*0}}{r} - 3. \tag{14}$$

The exact solution (13) is plotted in Figure 2, for different values of the polytropic exponent  $\gamma$ . Observe the enhanced acceleration of the solar wind caused by the polytropic gas effects, which is plausible because of enhanced flow expansion in the latter case.

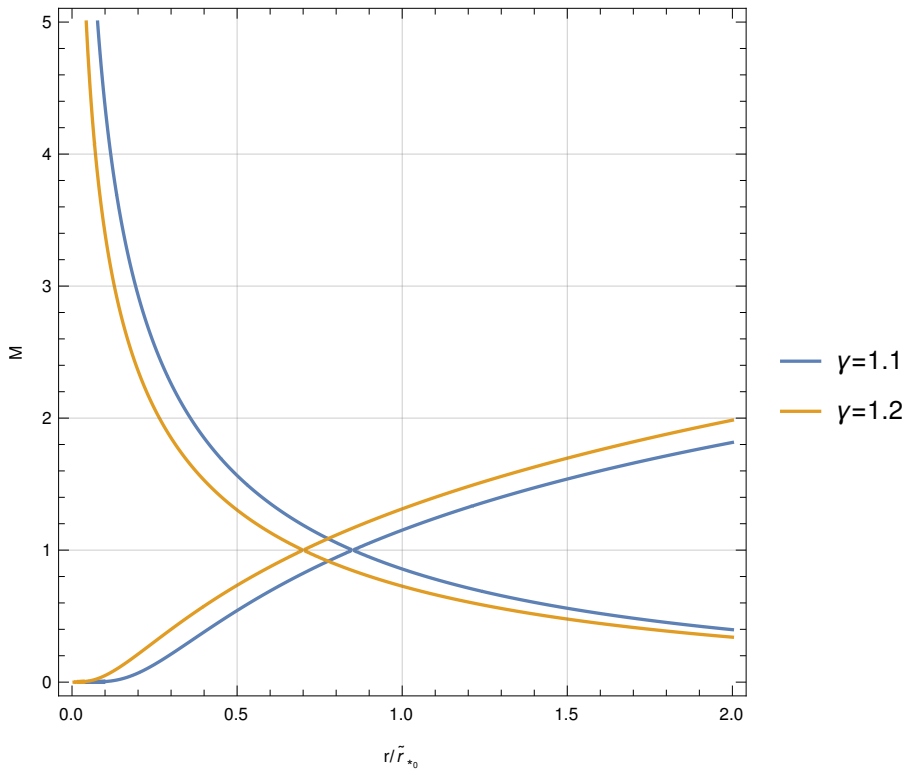


Figure 2: Exact solution (13) for the polytropic solar wind for two values of polytropic exponent  $\gamma$ .

### 3.1 Near-sun Regime

For  $r/\tilde{r}_{*0} \ll 1$ , (13) reduces to:

$$-\log M^2 \approx \frac{3\gamma - 5}{\gamma - 1} \log r, \quad (15a)$$

from which,

$$M^2 \sim r^{\frac{5-3\gamma}{\gamma-1}}. \quad (15b)$$

(15b) is valid, provided  $1 < \gamma < 5/3$ , which implies the coronal gas needs to be heated to achieve  $\gamma < 5/3$ .

On the other hand, in the isothermal gas limit ( $\gamma = 1$ ), (15b) is not valid, and (14) yields:

$$M^2 \sim e^{-4\frac{\tilde{r}_{*0}}{r}}. \quad (16)$$

Thus, any small deviation from the gas isothermality ( $\gamma \neq 1$ ) leads to a power-law (instead of an exponential law) enhancement of flow acceleration near the sun, so the power-law behavior given by (15b) needs to be taken as a more robust one. On the other hand, this signifies that the isothermal limit,  $\gamma \rightarrow 1$ , is a *singular* limit of the polytropic gas,  $\gamma > 1$ , so the polytropic gas results are not obtainable via a Taylor series expansion about the isothermal case.

### 3.2 Far-sun Regime

For  $r/\tilde{r}_{*0} \gg 1$ , (13) reduces to:

$$\left(-1 + \frac{\gamma + 1}{\gamma - 1}\right) \log M^2 \approx \left(\frac{3\gamma - 5}{\gamma - 1} + \frac{\gamma + 1}{\gamma - 1}\right) \log r, \quad (17a)$$

from which,

$$M^2 \sim r^{2(\gamma-1)}. \quad (17b)$$

On the other hand, in the isothermal gas limit ( $\gamma = 1$ ), (14) yields,

$$M^2 \sim \log r. \quad (18)$$

Thus, any small deviation from the gas isothermality ( $\gamma \neq 1$ ) leads to a power-law (instead of a logarithmic law) enhancement of flow acceleration far from the sun, so the power-law behavior given by (17b) needs to be taken again as a more robust one.

### 3.3 Transonic Regime

Near the Parker sonic critical point,  $r = r_* = \frac{5-3\gamma}{2} \tilde{r}_{*0}$ , we write,

$$r \equiv \frac{5-3\gamma}{2} \tilde{r}_{*0} + x, \quad M^2 \equiv 1 + y, \quad (19)$$

(13) then reduces to,

$$\begin{aligned} & -\log(1+y) + \frac{\gamma+1}{\gamma-1} \log\left(1 + \frac{\gamma-1}{\gamma+1} y\right) \\ & = -\frac{5-3\gamma}{\gamma-1} \log\left(1 + \frac{2}{5-3\gamma} \frac{x}{\tilde{r}_{*0}}\right) + \frac{\gamma+1}{\gamma-1} \log\left(1 + \frac{2}{\gamma+1} \frac{x}{\tilde{r}_{*0}}\right), \end{aligned}$$

and Taylor expanding in powers of  $y$  and  $x/\tilde{r}_{*0}$ , we obtain,

$$\frac{1}{\gamma+1} y^2 \approx \frac{1}{\gamma-1} \left( \frac{2}{5-3\gamma} - \frac{2}{\gamma+1} \right) \left( \frac{x}{\tilde{r}_{*0}} \right)^2,$$

from which,

$$y \approx \sqrt{\frac{8}{5-3\gamma}} \frac{x}{\tilde{r}_{*0}}, \quad (20a)$$

or

$$M^2 - 1 \approx \sqrt{\frac{8}{5-3\gamma}} \left( \frac{r}{\tilde{r}_{*0}} - \frac{5-3\gamma}{2} \right). \quad (20b)$$

(20a) and (20b) describe the asymptotes near the Parker sonic critical point ( $M^2 = 1$ ,  $r = \frac{5-3\gamma}{2} \tilde{r}_{*0}$ ) to the hyperbolas given by (13). This result implies that the Parker sonic critical point is of  $X$ -type, which facilitates a smooth transition from subsonic to supersonic wind flow through the transonic regime ( $M \approx 1$ ). Observe the enhancement in the flow acceleration past the Parker sonic critical point caused by the polytropic gas effects ( $\gamma > 1$ ).

It may be noted that the above asymptotic results (15b), (17b), (20b), for  $r/\tilde{r}_{*0} \ll 1$ ,  $r/\tilde{r}_{*0} \gg 1$ , and  $r \approx \frac{5-3\gamma}{2} \tilde{r}_{*0}$  may be deduced directly from equation (10) governing the polytropic gas flow (see Appendix A).

## 4 Coronal Hole Flows

The super-radial coronal-hole outflows involve rapidly diverging geometries and pose difficulties while considering them explicitly. In order to circumvent them, we will model the coronal-hole outflow by a magnetic-field aligned infinitesimal radial stream tube, and consider only a single stream tube because it would disrupt radial geometry for the neighboring stream tubes. Furthermore, the cross-sectional area  $A(r)$  of the stream tube appears in the equation governing the flow via only the ratio  $(1/A(r))(dA/dr)$ . So, one may, on phenomenological grounds, represent the rapidly-diverging flow geometry of the stream tube by taking the cross-sectional area  $A(r)$  to increase the outward from the sun faster than  $r^2$  (corresponding to a spherical geometry), as described by,

$$A(r) \sim r^\beta, \quad \beta > 2. \quad (21)$$

### 4.1 Isothermal Gas

Consider flow of isothermal gas in a stream tube of cross-sectional area  $A(r)$ . Equation (1) then becomes:

$$\frac{1}{\rho} \frac{d\rho}{dr} + \frac{1}{v_r} \frac{dv_r}{dr} + \frac{1}{A} \frac{dA}{dr} = 0. \quad (22)$$



Equations (2) and (22) lead to

$$\frac{1}{v_r} (v_r^2 - a^2) \frac{dv_r}{dr} = \frac{2a^2}{r^2} \left( \frac{r^2}{2A} \frac{dA}{dr} - r_* \right). \quad (23)$$

Using (21), equation (23) becomes,

$$\frac{1}{v_r} (v_r^2 - a^2) \frac{dv_r}{dr} = \beta \frac{a^2}{r^2} \left( r - \frac{2}{\beta} r_* \right). \quad (24)$$

Observe from equation (23) that the sonic critical point for a coronal-hole stream tube is given by

$$r = \frac{2}{\beta} r_* < r_* : v_r = a, \beta > 2 \quad (25)$$

which implies that the Parker sonic critical point occurs closer to the sun for a coronal-hole outflow ( $\beta > 2$ ).

Upon imposing the boundary condition (25), equation (24) yields the exact solution:

$$\frac{v_r^2}{a^2} - \log \left( \frac{v_r}{a} \right)^2 = 2\beta \log \left( \frac{\beta r}{2\tilde{r}_*} \right) + 4 \frac{r_*}{r} - (2\beta - 1). \quad (26)$$

In the radial-flow limit,  $\beta = 2$ , (26) reduces to the Parker solar wind solution (14).

## 4.2 Polytropic Gas

Consider next flow of a polytropic gas in a stream tube of cross-sectional area  $A(r)$ . Using equations (21) and (22), equations (10) and (11) become,

$$\begin{aligned} & \frac{M^2 - 1}{M^2 \left( 1 + \frac{\gamma-1}{2} M^2 \right)} \frac{dM^2}{dr} - (M^2 - 1) \left( \frac{4}{1 + 4 \frac{\gamma-1}{2} \frac{\tilde{r}_{*0}}{r}} \right) \\ &= \frac{4}{r^2} \left[ \frac{\beta}{2} r - \left( \frac{1 + \frac{\gamma-1}{2} M^2}{1 + 4 \frac{\gamma-1}{2} \frac{\tilde{r}_{*0}}{r}} \right) \tilde{r}_{*0} \right], \end{aligned} \quad (27)$$

or on simplification, the equation governing the super-radial polytropic gas flow becomes,

$$\frac{M^2 - 1}{M^2 \left( 1 + \frac{\gamma-1}{2} M^2 \right)} \frac{dM^2}{dr} = \frac{4}{r^2} \left( \frac{\beta}{2} r - \frac{\gamma + 1}{2} \frac{1}{1 + 4 \frac{\gamma-1}{2} \frac{\tilde{r}_{*0}}{r}} \tilde{r}_{*0} \right). \quad (28)$$

Observe from equation (28) that the Parker sonic critical point for a coronal-hole stream tube is given by,

$$M^2 = 1 : \frac{\beta}{2} r_* - \frac{\gamma + 1}{2} \frac{1}{1 + 4 \frac{\gamma-1}{2} \frac{\tilde{r}_{*0}}{r}} \tilde{r}_{*0} = 0,$$

or

$$M^2 = 1 : r_* = \frac{1}{\beta} [(2\beta + 1) - (2\beta - 1)\gamma] \tilde{r}_{*0}. \quad (29a)$$

Rewriting (29a) as,

$$r_* = \left[ 1 - \frac{1}{\beta} \left( \frac{\beta}{2} - 1 \right) (\gamma + 1) - \frac{3}{2} (\gamma - 1) \right] \tilde{r}_{*0}, \quad (29b)$$

and comparing with (12), super-radial flow conditions ( $\beta > 2$ ) are seen to cause the Parker sonic critical point to move further closer to the sun (see Figure 3) in a polytropic gas ( $\gamma > 1$ ). Furthermore, (29a) implies that

$$\gamma < \left( \frac{2\beta + 1}{2\beta - 1} \right) = \frac{5}{3} - \frac{4}{3} \left( \frac{\beta - 2}{2\beta - 1} \right) < \frac{5}{3}, \quad \beta > 2. \quad (29c)$$

So, in a super-radial flow, the gas is heated up even more to keep  $\gamma$  further below  $5/3$ .

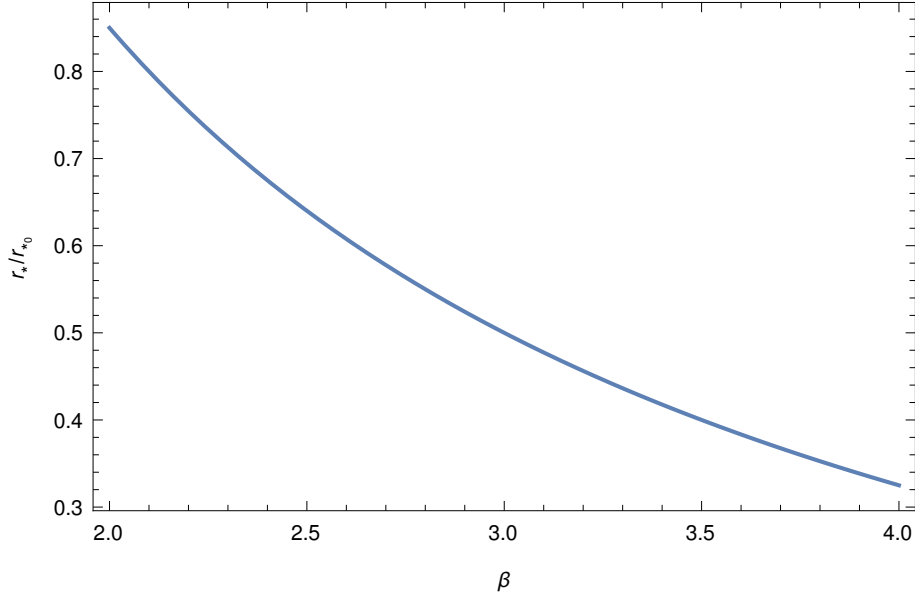


Figure 3: Super-radial flow effects, as per (29), on the Parker sonic critical point.

#### 4.2.1 Exact Solution

Upon imposing the boundary condition (29a), equation (28) yields the *exact* solution,

$$\begin{aligned} & -\log M^2 + \frac{\gamma + 1}{\gamma - 1} \log \left( \frac{1 + \frac{\gamma-1}{2} M^2}{\frac{\gamma+1}{2}} \right) \\ & = - \left( \frac{(2\beta + 1) - (2\beta - 1)\gamma}{\gamma - 1} \right) \log \left( \frac{\beta \left( \frac{r}{\tilde{r}_{*0}} \right)}{(2\beta + 1) - (2\beta - 1)\gamma} \right) \\ & + \frac{\gamma + 1}{\gamma - 1} \log \left( \frac{r + 4 \frac{\gamma-1}{2} \tilde{r}_{*0}}{\frac{2}{\beta} \frac{\gamma+1}{2} \tilde{r}_{*0}} \right). \end{aligned} \quad (30)$$

In the radial-flow limit,  $\beta = 2$ , (30) reduces to the polytropic gas solution (13), and in the isothermal gas limit,  $\gamma = 1$ , (30) reduces to (26).

The exact solution (30) is plotted in Figure 4, for different values of the super-radiality parameter  $\beta$ . Observe the enhanced acceleration of the coronal-hole outflows, which is plausible because of the enhanced flow expansion for such flows.

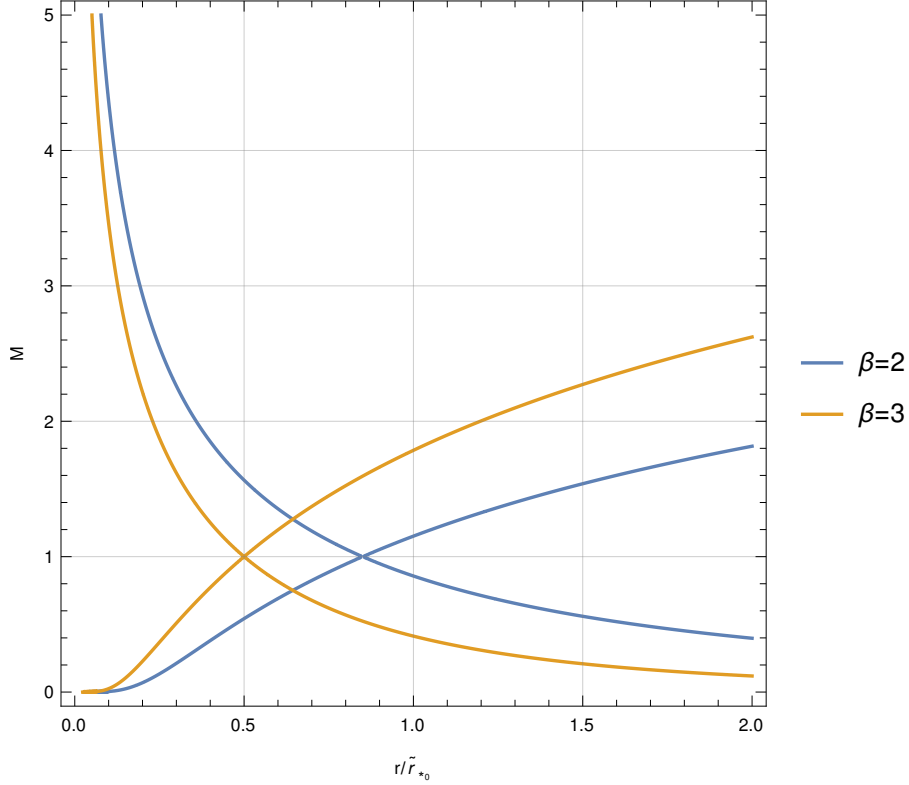


Figure 4: Exact solution (30) for a spherical radial expansion ( $\beta = 2$ ) and for super-radial expansion ( $\beta = 3$ ) of the polytropic solar wind.

#### 4.2.2 Near-sun Regime

For  $r/\tilde{r}_{*0} \ll 1$ , (30) reduces to,

$$\log M^2 \approx \left[ \frac{(2\beta + 1) - (2\beta - 1)\gamma}{\gamma - 1} \right] \log r, \quad (31a)$$

from which,

$$M^2 \sim r^{\frac{(2\beta+1)-(2\beta-1)\gamma}{\gamma-1}} \sim r^{\frac{5-3\gamma}{\gamma-1} - 2(\beta-2)}. \quad (31b)$$

On comparing with (15b), super-radial flow conditions,  $\beta > 2$ , are seen to cause an enhancement of flow acceleration near the sun.

### 4.2.3 Far-sun Regime

For  $r/\tilde{r}_{*0} \gg 1$ , (30) reduces to,

$$\left(-1 + \frac{\gamma+1}{\gamma-1}\right) \log M^2 \approx \left(\frac{(2\beta-1)\gamma - (2\beta+1)}{\gamma-1} + \frac{\gamma+1}{\gamma-1}\right) \log r, \quad (32a)$$

from which,

$$M^2 \sim r^{\beta(\gamma-1)}. \quad (32b)$$

On comparing with (17b), super-radial flow conditions,  $\beta > 2$ , are seen to cause an enhancement of flow acceleration also far away from the sun.

### 4.2.4 Transonic Regime

Near the Parker sonic critical point,  $r = r_* = \frac{(2\beta+1)-(2\beta-1)\gamma}{\beta} \tilde{r}_{*0}$ , we write,

$$r \equiv \frac{1}{\beta} [(2\beta+1) - (2\beta-1)\gamma] \tilde{r}_{*0} + x, \quad M^2 \equiv 1 + y. \quad (33)$$

(30) then reduces to,

$$\begin{aligned} & -\log(1+y) + \frac{\gamma+1}{\gamma-1} \log\left(1 + \frac{\gamma-1}{\gamma+1} y\right) \\ & = -\left(\frac{(2\beta+1) - (2\beta-1)\gamma}{\gamma-1}\right) \log\left[1 + \left(\frac{\beta}{(2\beta+1) - (2\beta-1)\gamma}\right) \frac{x}{\tilde{r}_{*0}}\right] \\ & + \frac{\gamma+1}{\gamma-1} \log\left(1 + \frac{\beta}{\gamma+1} \frac{x}{\tilde{r}_{*0}}\right), \end{aligned}$$

and Taylor expanding in powers of  $y$  and  $x/\tilde{r}_{*0}$ , we obtain,

$$y \approx \left(\frac{\beta^3}{(2\beta+1) - (2\beta-1)\gamma}\right)^{1/2} \frac{x}{\tilde{r}_{*0}}, \quad (34a)$$

which may be rewritten as,

$$y \approx \left(\frac{\beta^3}{(5-3\gamma) - 2(\beta-2)(\gamma-1)}\right)^{1/2} \frac{x}{\tilde{r}_{*0}}, \quad (34b)$$

or

$$M^2 - 1 \approx \left(\frac{\beta^3}{(5-3\gamma) - 2(\beta-2)(\gamma-1)}\right)^{1/2} \left(\frac{r}{\tilde{r}_{*0}} - \frac{(2\beta+1) - (2\beta-1)\gamma}{\beta}\right). \quad (34c)$$

(34) describe the asymptotes near the Parker sonic critical point ( $M^2 = 1$ ,  $r = \frac{(2\beta+1)-(2\beta-1)\gamma}{\beta} \tilde{r}_{*0}$ ) to the hyperbolas given by (30). This result, as in the radial-flow case ( $\beta = 2$ ), implies that the Parker sonic critical point is of  $X$ -type, which facilitates a smooth transition from subsonic to supersonic wind flow through the transonic regime ( $M \approx 1$ ). Observe the enhancement in the flow acceleration past the Parker sonic critical point caused by super-radial flow conditions ( $\beta > 2$ ).

It may be noted that the above asymptotic results (31), (32), and (34), for  $r/\tilde{r}_{*0} \ll 1$ ,  $r/\tilde{r}_{*0} \gg 1$  and  $r \approx \frac{(2\beta+1)-(2\beta-1)\gamma}{\beta} \tilde{r}_{*0}$  may be deduced directly from equation (28) governing the super-radial, polytropic gas flow (see Appendix B).

## 5 Discussion

In recognition of the impairment of the isothermal gas assumption in Parker's solar wind model due to extended active heating in the corona, we have given a detailed and systematic investigation of polytropic gas effects in Parker's model. We have presented a viable equation governing the acceleration of the solar wind of a polytropic gas, and have given its analytical and numerical solutions, and have exhibited its asymptotic analytic properties (i) near the sun, (ii) far away from the sun, (iii) near the Parker sonic critical point (where the wind speed is equal to the speed of sound in the wind). On the other hand, the bulk of the solar wind is found to emerge from the coronal holes, so we have given a detailed and systematic investigation of coronal-hole polytropic gas outflows. We have modeled coronal-hole outflow by considering a single radial stream tube and used phenomenological considerations to represent its rapidly diverging flow geometry. We have given *exact analytical* and numerical solutions for this outflow and exhibited its asymptotic analytic properties in the three flow regimes listed above. We have found that, in general, the polytropic effects cause the Parker sonic critical point to move closer to the sun than that for the case with isothermal gas. Furthermore, the flow acceleration has been found to exhibit (even for an infinitesimal deviation from isothermality of the gas) a power-law behavior rather than an exponential-law behavior near the sun or a logarithmic-law behavior far away from the sun, thus implying a certain robustness of the power-law behavior for the flow acceleration. This also signifies that the isothermal limit,  $\gamma \rightarrow 1$ , is a *singular* limit of the polytropic gas,  $\gamma > 1$ , so the polytropic gas results are not obtainable via a Taylor series expansion about the isothermal case. Parker sonic critical point has been shown to continue to be of *X*-type, hence, facilitating a smooth transition from subsonic to supersonic wind flow through the transonic regime. Our analytical and numerical solutions show that the super-radiality of the stream tube causes the Parker sonic critical point to move further down in the corona, and the gas to become more diabatic (the polytropic exponent  $\gamma$  drops further below  $5/3$ ), and the flow acceleration to be enhanced in agreement with numerical calculations of Kopp and Holzer (1976).

## 6 Acknowledgements

This work was carried out during BKS's sabbatical leave at California Institute of Technology. BKS thanks Professor Shrinivas Kulkarni for his enormous hospitality and valuable remarks and Drs. Elias Most and Reem Sari for the helpful discussions. BKS is thankful to o Professors Earl Dowell and Katepalli Screenivasan for their helpful remarks and suggestions.

## Appendix A

### A.1 Near-sun Regime

For  $r/\tilde{r}_{*0} \ll 1$ , equation (11) reduces to,

$$-\frac{1}{M^2} \frac{dM^2}{dr} \approx \frac{4}{r^2} \left( r - \frac{\tilde{r}_{*0}}{4} \frac{\gamma+1}{\gamma-1} \frac{r}{\tilde{r}_{*0}} \right), \quad (\text{A.1})$$

or

$$\frac{d(\log M^2)}{dr} \approx \frac{5-3\gamma}{\gamma-1} \frac{1}{r}, \quad (\text{A.2})$$

from which

$$M^2 \sim r^{\frac{5-3\gamma}{\gamma-1}}, \quad (\text{A.3})$$

in agreement with (15b).

### A.2 Far-Star Regime

For  $r/\tilde{r}_{*0} \gg 1$ , equation (11) reduces to,

$$\frac{2}{\gamma-1} \frac{dM^2}{dr} \approx \frac{4}{r}, \quad (\text{A.4})$$

from which,

$$M^2 \sim r^{2(\gamma-1)}, \quad (\text{A.5})$$

in agreement with (17b).

### A.3 Transonic Regime

Near the Parker sonic critical point  $r = r_* = \frac{5-3\gamma}{2} \tilde{r}_{*0}$ , we write,

$$r \equiv \frac{5-3\gamma}{2} \tilde{r}_{*0} + x, \quad M^2 \equiv 1 + y, \quad (\text{A.6})$$

equation (11) then reduces to,

$$\begin{aligned} & \frac{y}{(1+y) \left[ 1 + \frac{\gamma-1}{2} (1+y) \right]} \frac{dy}{dr} \\ &= \frac{4}{\left( \frac{5-3\gamma}{2} \tilde{r}_{*0} + x \right)^2} \left[ \left( \frac{5-3\gamma}{2} \tilde{r}_{*0} + x \right) - \frac{\gamma+1}{2} \frac{\tilde{r}_{*0}}{1 + \frac{2(\gamma-1)\tilde{r}_{*0}}{\frac{5-3\gamma}{2} \tilde{r}_{*0} + x}} \right], \end{aligned} \quad (\text{A.7})$$

and Taylor expanding in powers of  $y$  and  $x/\tilde{r}_{*0}$ , we obtain,

$$\begin{aligned} \frac{2y}{\gamma+1} \frac{dy}{dr} &\approx \frac{16}{(5-3\gamma)^2 \tilde{r}_{*0}} \left[ \left( \frac{5-3\gamma}{2} - \frac{\gamma+1}{2} \frac{1}{1 + 4 \frac{\gamma-1}{5-3\gamma}} \right) \right. \\ &\quad \left. + \left( \frac{5-3\gamma}{2} - 2 \frac{\gamma^2-1}{5-3\gamma} \frac{1}{\left( 1 + 4 \frac{\gamma-1}{5-3\gamma} \right)^2} \right) \frac{2}{5-3\gamma} \frac{x}{\tilde{r}_{*0}} \right], \end{aligned} \quad (\text{A.8})$$

or

$$y \frac{dy}{dr} \approx \frac{8}{5-3\gamma} \frac{x}{\tilde{r}_{*0}^2}, \quad (\text{A.9})$$

from which we obtain

$$y \approx \sqrt{\frac{8}{5-3\gamma}} \frac{x}{\tilde{r}_{*0}}, \quad (\text{A.10})$$

in agreement with (20a).

## Appendix B

### B.1 Near-sun Regime

For  $r/\tilde{r}_{*0} \ll 1$ , equation (28) reduces to,

$$-\frac{dM^2}{dr} \approx \frac{4}{r^2} \left( \frac{\beta}{2} r - \frac{\tilde{r}_{*0}}{4} \frac{\gamma+1}{\gamma-1} \frac{r}{\tilde{r}_{*0}} \right), \quad (\text{B.1})$$

or

$$\frac{d(\log M^2)}{dr} \approx \frac{(2\beta+1) - (2\beta-1)\gamma}{\gamma-1} \frac{1}{r}, \quad (\text{B.2})$$

from which,

$$M^2 \sim r^{\frac{(2\beta+1)-(2\beta-1)\gamma}{\gamma-1}}, \quad (\text{B.3})$$

in agreement with (31b).

### B.2 Far-sun Regime

For  $r/\tilde{r}_{*0} \gg 1$ , equation (28) reduces to,

$$\frac{2}{\gamma-1} \frac{dM^2}{dr} \approx \frac{2\beta}{r}, \quad (\text{B.4})$$

from which,

$$M^2 \sim r^{\beta(\gamma-1)}, \quad (\text{B.5})$$

in agreement with (32b).

### B.3 Transonic Regime

Near the Parker sonic critical point  $r = r_* = \left( \frac{(2\beta+1)-(2\beta-1)\gamma}{\beta} \right) \tilde{r}_{*0}$ , we write,

$$r \equiv \frac{(2\beta+1) - (2\beta-1)\gamma}{\beta} \tilde{r}_{*0} + x, \quad M^2 \equiv 1 + y, \quad (\text{B.6})$$

equation (28) then reduces to,

$$\begin{aligned} & \frac{y}{(1+y) \left[ 1 + \frac{\gamma-1}{2}(1+y) \right]} \frac{dy}{dr} \\ &= \frac{4}{\left( \left( \frac{(2\beta+1)-(2\beta-1)\gamma}{\beta} \right) \tilde{r}_{*0} + x \right)^2} \left[ \frac{\beta}{2} \left( \left( \frac{(2\beta+1)-(2\beta-1)\gamma}{\beta} \right) \tilde{r}_{*0} + x \right) \right. \\ & \left. - \frac{\gamma+1}{2} \frac{\tilde{r}_{*0}}{1 + \frac{2(\gamma-1)\tilde{r}_{*0}}{\left( \frac{(2\beta+1)-(2\beta-1)\gamma}{\beta} \right) \tilde{r}_{*0} + x}} \right], \end{aligned} \quad (\text{B.7})$$

and Taylor expanding in powers of  $y$  and  $x/\tilde{r}_{*0}$ , we obtain,

$$\begin{aligned} \frac{2y}{\gamma+1} \frac{dy}{dr} &\approx \frac{4}{\left( \frac{(2\beta+1)-(2\beta-1)\gamma}{\beta} \right)^2 \tilde{r}_{*0}^2} \times \\ &\times \left[ \frac{\beta}{2} - \frac{\gamma^2 - 1}{\left\{ \frac{1}{\beta} [(2\beta+1) - (2\beta-1)\gamma] + 2(\gamma-1) \right\}^2} \right] x, \end{aligned} \quad (\text{B.8})$$

or

$$y \frac{dy}{dr} \approx \left[ \frac{\beta^3}{(2\beta+1) - (2\beta-1)\gamma} \right] \frac{x}{\tilde{r}_{*0}^2}, \quad (\text{B.9})$$

from which we obtain

$$y \approx \left[ \frac{\beta^3}{(2\beta+1) - (2\beta-1)\gamma} \right]^{1/2} \frac{x}{\tilde{r}_{*0}}, \quad (\text{B.10})$$

in agreement with (34a).

## References

- Altschuler, M. D., Trotter, D. E., and Orrall, F. Q. (Oct. 1, 1972). “Coronal Holes”. In: *Solar Physics* 26.2, pp. 354–365. ISSN: 1573-093X.
- Bale, S. D. et al. (June 7, 2023). “Interchange Reconnection as the Source of the Fast Solar Wind within Coronal Holes”. In: *Nature* 618.7964, pp. 252–256. ISSN: 1476-4687. pmid: 37286648.
- Boldyrev, S., Forest, C., and Egedal, J. (Apr. 28, 2020). “Electron Temperature of the Solar Wind”. In: *Proceedings of the National Academy of Sciences* 117.17, pp. 9232–9240.
- Bondi, H. (Apr. 1, 1952). “On Spherically Symmetrical Accretion”. In: *Monthly Notices of the Royal Astronomical Society* 112.2, pp. 195–204. ISSN: 0035-8711.
- Fisk, L. A. and Kasper, J. C. (Apr. 2020). “Global Circulation of the Open Magnetic Flux of the Sun”. In: *The Astrophysical Journal Letters* 894.1, p. L4. ISSN: 2041-8205.
- Holzer, T. E. (1979). “The Solar Wind and Related Astrophysical Phenomena”. In: *Solar System Plasma Physics*. Ed. by C. F. Kennel, L. J. Lanzerotti, and E. N. Parker. Amsterdam-New York-Oxford: North-Holland Publishing Company, pp. 101–176.



- Kasper, J. C. et al. (Dec. 12, 2019). “Alfvénic Velocity Spikes and Rotational Flows in the Near-Sun Solar Wind”. In: *Nature* 576.7786, pp. 228–231. ISSN: 14764687. pmid: 31802006.
- Keppens, R. and Goedbloed, J. P. (1999). “Numerical Simulations of Stellar Winds”. In: *Coronal Holes and Solar Wind Acceleration*. Dordrecht: Springer Netherlands, pp. 223–226.
- Kopp, R. A. and Holzer, T. E. (July 1976). “Dynamics of Coronal Hole Regions - I. Steady Polytopic Flows with Multiple Critical Points”. In: *Solar Physics* 49.1, pp. 43–56. ISSN: 00380938.
- Krieger, A. S., Timothy, A. F., and Roelof, E. C. (Apr. 1, 1973). “A Coronal Hole and Its Identification as the Source of a High Velocity Solar Wind Stream”. In: *Solar Physics* 29.2, pp. 505–525. ISSN: 1573-093X.
- Meyer-Vernet, N. (2007). *Basics of the Solar Wind*. Cambridge Atmospheric and Space Science Series. Cambridge: Cambridge University Press. ISBN: 978-0-521-81420-1.
- Nolte, J. T. et al. (Feb. 1, 1976). “Coronal Holes as Sources of Solar Wind”. In: *Solar Physics* 46.2, pp. 303–322. ISSN: 1573-093X.
- Parker, E. N. (Nov. 1958). “Dynamics of the Interplanetary Gas and Magnetic Fields.” In: *The Astrophysical Journal* 128, p. 664. ISSN: 0004-637X.
- (Nov. 1, 1960). “The Hydrodynamic Theory of Solar Corpuscular Radiation and Stellar Winds.” In: *The Astrophysical Journal* 132, p. 821. ISSN: 0004-637X.
- (Aug. 1, 1971). “Recent Developments in Theory of Solar Wind”. In: *Reviews of Geophysics* 9.3, pp. 825–835. ISSN: 19449208.
- Sakao, T. et al. (Dec. 7, 2007). “Continuous Plasma Outflows from the Edge of a Solar Active Region as a Possible Source of Solar Wind”. In: *Science* 318.5856, pp. 1585–1588. ISSN: 00368075.
- Shivamoggi, B. K. (Jan. 2020). “Stellar Rotation Effects on the Stellar Winds”. In: *Physics of Plasmas* 27.1, p. 012902. ISSN: 10897674.
- Shivamoggi, B. K., Rollins, D. K., and Pohl, L. (Nov. 12, 2021). “Parker’s Solar Wind Model for a Polytopic Gas”. In: *Entropy* 23.11, p. 1497. ISSN: 10994300.
- Wang, Y. M. and Sheeley Jr., N. R. (June 1, 1990). “Solar Wind Speed and Coronal Flux-Tube Expansion”. In: *The Astrophysical Journal* 355, p. 726. ISSN: 0004-637X.